We are IntechOpen, the world's leading publisher of Open Access books Built by scientists, for scientists

4,800
Open access books available

122,000
International authors and editors

135M
Downloads

Our authors are among the

154
Countries delivered to

TOP 1%
most cited scientists

12.2%
Contributors from top 500 universities

CLARIVATE ANALYTICS BOOK CITATION INDEX INDEXED

WEB OF SCIENCE™

Selection of our books indexed in the Book Citation Index in Web of Science™ Core Collection (BKCI)

Interested in publishing with us?
Contact book.department@intechopen.com

Numbers displayed above are based on latest data collected.
For more information visit www.intechopen.com

Chapter 2

Excitons and Trions in Semiconductor Quantum Dots

S. A. Safwan and N. El–Meshed

Additional information is available at the end of the chapter

http://dx.doi.org/10.5772/61177

Abstract

We aim from this chapter to declare for the readers, what are the exciton and trions in quantum dot and we will present complete theoretical discussion for the behavior of exciton ,its bound state ,binding energy and its stability in quantum dot with different sizes and different confinement potentials .The charged complex particles as negative and positive trions will be investigated theoretically using variational procedure in both strong and weak confinement regime . Good agreement with experimental data was found and discussed.

Keywords: quantum dot, exciton, trion, binding energy

1. Introduction

During the optical excitation of carriers in a semiconductor, the minimum energy required to form free carriers is called the band gap. The energy below that value cannot excite free carriers. However, low-temperature absorption studies of semiconductors have shown excitation just below the band gap [1]. This excitation is associated with the formation of an electron and an electron hole bound to each other, otherwise called an exciton. It is an electrically neutral quasiparticle like in a hydrogenic state. At low temperatures, the bound states are formed and the Coulomb interaction between the electron and the hole becomes prominent [2]. The negative trion (X-) is created due to the additional electron bound to a pre-existing exciton and if a hole is bound to an exciton, a positive trion (X^+) is created. Both the negative and positive trions are complex electronic excited states of the

semiconductors and therefore, the 3-body problem is raised. Although Lampert [3] in 1958 originally and theoretically predicted the negative trion in semiconductors, K.Kheng et al. experimentally achieved a negative trion in Cd Te/Cd Zn Te quantum well [4].

The rapid progress of semiconductor technology in the recent years has allowed the fabrication of low dimension electronic nanostructures. Such nanostructures confine charged particles in all three space dimensions. In low dimensional, especially in quantum dots [5,6] (three dimension confinement), the picture is different because it is below a nanometer wide, a few nanometers thick, and in various shapes. The quantum confinement increases highly, and this quantum confinement leads to more stability of the excitons and trions by increasing their binding energy. The stability of such particles remains up to room temperature. A proper identification of the (X-) was not achieved until the early 1990's in remotely doped, high-quality quantum-well (QW) structures [7-9]. Since then, extensive work has been carried out on (X-) inside the two-dimensional (2D) [wide quantum wells [7-11]] and quantum dots, which the first observations of the QD-confined charged excitons (trions) were performed on ensembles of the QDs [12]. There are many theoretical studies devoted to excitons [13-15] and trions [16-25] in quantum dot. Most of such studies have treated and considered the spherical[26-28], lens shaped [29,30], square flat plated [31,32], and cylindrical [33,34] quantum dots.

In the present chapter, we study the influence of the 3-D quantum confinement on the binding energy of the exciton (X), negative trion (X-), and the positive trion (X^+) in a semiconductor cylindrical quantum dot manufactured in GaAs surrounded by $Ga_{1-x}Al_xAs$. Using a variational approach and the effective mass approximation with finite confinement – potential. There have been concerns as to whether the effective mass approximation could still be valid in the quantum dot limit when the size of the exciton could be similar to the average lattice constants of bulk semiconductor [35].

2. Theoretical model

Within the effective mass approximation and non-degenerated band approximation, we can describe the exciton and trions in the following semiconductor structure: a symmetric cylindrical QD of radius R and height L made of GaAs surrounded by $Ga_{1-x}Al_xAs$. In our model, the electrons and the holes are placed in the external potential $V_e(r_e, z_e)$ and $V_h(r_h, z_h)$, respectively and coupled via Coulomb potential. We choose the potential in GaAs (well) to be zero and equals V_e or V_h in the barrier material.

2.1. Exciton

The Hamiltonian of an exciton confined in cylindrical QD, using the relative coordinate $r = |\bar{r}_e - \bar{r}_h|$, can be written as[36]:

http://dx.doi.org/10.5772/61177

$$H = \frac{-\hbar^2}{2m^*_e}\left\{\frac{\partial^2}{\partial r_e^2}+\frac{1}{r_e}\frac{\partial}{\partial r_e}+\frac{r_e^2-r_h^2+r^2}{r_e r}\frac{\partial^2}{\partial r_e \partial r}+\frac{\partial^2}{\partial z_e^2}\right\}$$
$$\frac{-\hbar^2}{2m^*_h}\left\{\frac{\partial^2}{\partial r_h^2}+\frac{1}{r_h}\frac{\partial}{\partial r_h}+\frac{r_h^2-r_e^2+r^2}{r_h r}\frac{\partial^2}{\partial r_h \partial r}+\frac{\partial^2}{\partial z_h^2}\right\} \quad (1)$$
$$\frac{-\hbar^2}{2\mu}\left\{\frac{\partial^2}{\partial r^2}+\frac{1}{r}\frac{\partial}{\partial r}\right\}+V_e(r_e,z_e)+V_h(r_h,z_h)-\frac{e^2}{\varepsilon_0\varepsilon\sqrt{(r_e-r_h)^2+(z_e-z_h)^2}}$$

Where m^*_e and m^*_h is the effective mass of the electron and the hole, respectively, μ is the reduced mass of exciton $\mu = m_e\, m_h / m_e + m_h$, and ($r_e$, z_e) and (r_h, z_h) are the spatial coordinates of the electrons and hole in the cylindrical frame, respectively. The first three terms of equation (1) represent the kinetic energy of the electron, hole, and exaction's center of mass existing in the structure under consideration. The last three terms represent the confinement potentials followed by the Coulomb interaction term. ε is the relative static dielectric constant for the used material and ε_0 is the permittivity of free space. We can write the expressions of $V_e(r_e, z_e)$ and $V_h(r_h, z_h)$ as:

$$\mathrm{V}(\mathrm{r_i},\mathrm{z_i}) = \begin{cases} 0 & \mathrm{r_i} \le \mathrm{R \text{ and } } |\mathrm{z_i}| \le \mathrm{L} \\ \mathrm{V_o} & \mathrm{r_i} > \mathrm{R \text{ and } } |\mathrm{z_i}| > L \end{cases} \quad (2)$$

Here the indices i stand for the electron (e) or the hole (h).

The Schrödinger equation for the exciton in the quantum dot is:

$$H\Psi\left(r_e, r_h, r, z_e, z_h\right) = E\Psi\left(r_e, r_h, r, z_e, z_h\right) \quad (3)$$

By choosing the following trial wave function, it takes into account the electron–hole correlation and the Ritz variation principle that are used to solve this equation. Thoroughly, we are able to determine the exciton ground state (E_{ex}),

$$\Psi(r_e, r_h, r_{eh}, z_e, z_h) = f(r_e)\, f(r_h) g(z_e) g(z_h) \exp\left(-\alpha\sqrt{(r_e-r_h)^2+\left(z_e-z_h\right)^2}\right) \quad (4)$$

The variation parameter α is determined by minimizing the value of the exciton energy:

$$E_{ex}(\alpha) = \langle\Psi|H|\Psi\rangle / \langle\Psi|\Psi\rangle, \quad (5)$$

The binding energy of the exciton is given by:

$$E_b = E_e + E_h - E_{ex} \tag{6}$$

Where $f(r_e)$, $f(r_h)$, $g(z_e)$, $g(z_h)$ and E_e, E_h are the ground wave functions and energies of both the electron and the hole [37].

2.2. Negative trion

The negative trion (X-) is created when an additional electron is bound to a pre-existing exciton (X). The negative trion Hamiltonian in a cylindrical coordinate can be written as:

$$\begin{aligned} H = & \frac{-\hbar^2}{2m^*_e}\left\{\frac{\partial^2}{\partial r_{e_1}^2}+\frac{1}{r_{e_1}}\frac{\partial}{\partial r_{e_1}}+\frac{\partial^2}{\partial z_{e_1}^2}\right\}\frac{-\hbar^2}{2m^*_e}\left\{\frac{\partial^2}{\partial r_{e_2}^2}+\frac{1}{r_{e_2}}\frac{\partial}{\partial r_{e_2}}+\frac{\partial^2}{\partial z^2_{e_2}}\right\} \\ & \frac{-\hbar^2}{2m^*_h}\left\{\frac{\partial^2}{\partial r_h^2}+\frac{1}{r_h}\frac{\partial}{\partial r_h}+\frac{\partial^2}{\partial z_h^{\,2}}\right\}+V_{e_1}(r_{e_1},z_{e_1})+V_h(r_h,z_h)+V_{e_2}(r_{e_2},z_{e_2}) \\ & +\frac{e^2}{4\pi\varepsilon_0\varepsilon}\left[\frac{1}{\sqrt{(r_{e_1}-r_{e_2})^2+(z_{e_1}-z_{e_2})^2}}-\frac{1}{\sqrt{(r_{e_1}-r_h)^2+(z_{e_1}-z_h)^2}}-\frac{1}{\sqrt{(r_{e_2}-r_h)^2+(z_{e_2}-z_h)^2}}\right] \end{aligned} \tag{7}$$

The first three terms of equation (7) represent the kinetic energy terms of the three particles existing in the structure under consideration. The second three terms represent the confinement potentials followed by the three Coulomb interaction terms. We use equation (2) for expressions of $V_e(r_e, z_e)$ and $V_h(r_h, z_h)$.

The present model is fully three dimensional and is applicable to the confinement potentials of finite range and depth, i.e., it is adequate for QD nano-crystals embedded in an insulating medium, e.g. GaAs [38] and InAs [39, 40]. The quantum well potential given above does not commute with the kinetic energy operator at the center of the mass motion. Therefore, the Hamiltonian (7) cannot be separated from the center of the mass and Hamiltonians of the relative motion.

The full three dimension Schrödinger equation for the negative trion in quantum dot is:

$$H\,\Psi\left(r_{e_1}, r_{e_2}, r_h, z_{e_1}, z_{e2}, z_h\right) = E\,\Psi\left(r_{e_1}, r_{e_2}, r_h, z_{e_1}, z_{e_2}, z_h\right) \tag{8}$$

Hence, the ground state wave function for the negative trion confined in the cylindrical quantum dot has dependent on the six coordinate parameters appearing in equation (8). Here, we adopt the variation approach to estimate the ground state of the negative trions (X-), their binding energy, and their wave functions. We choose the following trial wave function:

http://dx.doi.org/10.5772/61177

$$\Psi_{trion} = f\left(r_{e_1}\right) f\left(r_{e_2}\right) f\left(r_h\right) g\left(z_{e_1}\right) g\left(z_{e_2}\right) g\left(z_h\right) \varphi\left(r_{e_1}, r_{e_2}, r_h, z_{e_1}, z_{e_2}, z_h\right) \tag{9}$$

Where, $f(r_{e_1})$, $f(r_{e_2})$, $f(r_h)$, $g(z_{e_1})$, $g(z_{e_2})$ *and* $g(z_h)$ are the single particle eigenfunctions [37], and the trial wave function ϕ describes the internal motion of the trions (X-) defined as:

$$\phi(r_{e_1}, r_{e_2}, r_h, z_{e_1}, z_{e_2}, z_h) = \exp\left[\begin{array}{l} -\left(\beta_1 \sqrt{(r_h - r_{e_1})^2 + (z_h - z_{e_1})^2}\right) - \left(\beta_2 \sqrt{(r_h - r_{e_2})^2 + (z_h - z_{e_2})^2}\right) \\ -\left(\beta_3 \sqrt{(r_{e_1} - r_{e_2})^2 + (z_{e_1} - z_{e_2})^2}\right) \end{array}\right]$$

Here β_1, β_2 *and* β_3 are the variation parameters. The form of the wave function given in equation (9) satisfies not only the strong interaction region requirements (such as in a very narrow quantum dots), but also yields the correct results near the bulk limits (weak interaction region).

Let $\chi_{e_1} = \frac{r_{e_1}}{R}$, $\chi_{e_2} = \frac{r_{e_2}}{R}$, $\chi_h = \frac{r_h}{R}$ *and* $\varsigma_{e_1} = \frac{z_{e_1}}{L}$, $\varsigma_{e_2} = \frac{z_{e_2}}{L}$, $\varsigma_h = \frac{z_h}{L}$,

where $0 \le \chi_i \le 1$ and $-1 \le \varsigma_i \le 1$. Now, we rewrite the arguments of the negative trion wave functions in terms of χ's , *and* ς's and define, $\chi_1 = |\chi_h - \chi_{e_1}|$, $\chi_2 = |\chi_{e_2} - \chi_h|$, $\chi_3 = |\chi_{e_1} - \chi_{e_2}|$ and $\varsigma_1 = (\varsigma_h - \varsigma_{e_1})$, $\varsigma_2 = (\varsigma_{e_2} - \varsigma_{h_1})$, $\varsigma_3 = (\varsigma_{e_1} - \varsigma_{e_2})$,

By using the new variables, the trial wave function can be expressed as follows:

$$\begin{aligned} &\psi_{trion}\left(\chi_{e_1}, \chi_{e_2}, \chi_h, \varsigma_{e_1}, \varsigma_{e_2}, \varsigma_h\right) = f\left(\chi_{e_1}\right) f\left(\chi_{e_2}\right) f\left(\chi_h\right) g\left(\zeta_{e_1}\right) g\left(\zeta_{e2}\right) g\left(\zeta_h\right) \\ &\times \exp\left[-\left(\beta_1 \sqrt{R^2 \chi_1^{\,2} + L^2 \varsigma_1}\right) - \left(\beta_2 \sqrt{R^2 \chi_2^{\,2} + L^2 \varsigma_2^{\,2}}\right) - \left(\beta_3 \sqrt{R^2 \chi_3^{\,2} + L^2 \varsigma_3^{\,2}}\right)\right] \end{aligned} \tag{10}$$

The ground state energy of the charged exciton system is given by:

$$\left\langle E_{trion}(\beta_1, \beta_2\ , \beta_3)\right\rangle = \frac{\left\langle \psi_{trion} \middle| H \middle| \psi_{trion} \right\rangle}{\left\langle \psi_{trion} \middle| \psi_{trion} \right\rangle} \tag{11}$$

Following some tedious algebra to minimize the above equation with respect to the variational parameters β_1, β_2 *and* β_3, we obtained the ground state energy of the negative trion. The variational method is used to calculate the ground state of the negative and positive trions.

The integral form of the nominator in the R.H.S of equation (11) is:

$$\left\langle \Psi_{trion} \middle| H \middle| \Psi_{trion} \right\rangle = \int_{-\infty}^{\infty}\int_{-\infty}^{\infty}\int_{-\infty}^{\infty}\int_{0}^{\infty}\int_{0}^{\infty}\int_{0}^{\infty}\int_{0}^{\infty} \Psi^{*} H \Psi \, r_{e_1} dr_{e_1} \, r_{e_2} dr_{e_2} r_h dr_h \, dz_{e_1} dz_{e_2} dz_h \tag{12}$$

Considering the following mathematical formula which is proven in Appendix:

$$-\int_{0}^{\infty} \Psi^{*} \left\{ \frac{d^2}{dr^2} + \frac{1}{r}\frac{d}{dr} \right\} \psi \, r dr = \int_{0}^{\infty} \left(\frac{d\psi}{dr} \right)^2 r dr \tag{13}$$

The equation (12) is presented in terms of $\chi's$, *and* $\zeta's$ as:

$$\begin{aligned}
&\left\langle \Psi_{trion} \middle| H \middle| \Psi_{trion} \right\rangle = \\
&= \int_{-1}^{1}\int_{-1}^{1}\int_{-1}^{1}\int_{0}^{1}\int_{0}^{1}\int_{0}^{1} f^2(\chi_{e_1}) f^2(\chi_{e_2}) f^2(\chi_h) g^2(\varsigma_{e_1}) g^2(\varsigma_{e2}) g^2(\varsigma_h) [\varphi(\chi_{e_1}, \chi_{e_2}, \chi_h, \varsigma_{e_1}, \varsigma_{e_2}, \varsigma_h)]^2 \\
&\times \left\{ \frac{\hbar^2}{2m^*_e R^2} \left[\left(\frac{f'(\chi_{e_1})}{f(\chi_{e_1})} \right) + \frac{\beta_1 R^2 \chi_1}{\sqrt{R^2\chi_1^2 + L^2\varsigma_1^2}} - \frac{\beta_3 R^2 \chi_3}{\sqrt{R^2\chi_3^2 + L^2\varsigma_3^2}} \right]^2 \right. \\
&+ \frac{\hbar^2}{2m^*_e R^2} \left[\left(\frac{f'(\chi_{e_2})}{f(\chi_{e_2})} \right) - \frac{\beta_2 R^2 \chi_2}{\sqrt{R^2\chi_2^2 + L^2\varsigma_2^2}} + \frac{\beta_3 R^2 \chi_3}{\sqrt{R^2\chi_3^2 + L^2\varsigma_3^2}} \right]^2 \\
&+ \frac{\hbar^2}{2m^*_h R^2} \left[\left(\frac{f'(\chi_h)}{f(\chi_h)} \right) - \frac{\beta_1 R^2 \chi_1}{\sqrt{R^2\chi_1^2 + L^2\varsigma_2^2}} + \frac{\beta_2 R^2 \chi_2}{\sqrt{R^2\chi_2^2 + L^2\varsigma_2^2}} \right]^2 \\
&+ \frac{\hbar^2}{2m^*_e L^2} \left[\left(\frac{g'(\varsigma_{e_1})}{g(\varsigma_{e_1})} \right) + \frac{\beta_1 L^2 \varsigma_1}{\sqrt{R^2\chi_1^2 + L^2\varsigma_1^2}} - \frac{\beta_3 L^2 \varsigma_3}{\sqrt{R^2\chi_3^2 + L^2\varsigma_3^2}} \right]^2 \\
&+ \frac{\hbar^2}{2m^*_e L^2} \left[\left(\frac{g'(\varsigma_{e_2})}{g(\varsigma_{e_2})} \right) - \frac{\beta_2 L^2 \varsigma_2}{\sqrt{R^2\chi_2^2 + L^2\varsigma_2^2}} + \frac{\beta_3 L^2 \varsigma_3}{\sqrt{R^2\chi_3^2 + L^2\varsigma_3^2}} \right]^2 \\
&+ \frac{\hbar^2}{2m^*_h L^2} \left[\left(\frac{g'(\varsigma_h)}{g(\varsigma_h)} \right) - \frac{\beta_1 L^2 \varsigma_1}{\sqrt{R^2\chi_1^2 + L^2\varsigma_1^2}} + \frac{\beta_2 L^2 \varsigma_2}{\sqrt{R^2\chi_2^2 + L^2\varsigma_2^2}} \right]^2 \\
&+ V_{e_1}(\chi_{e_1}, \varsigma_{e_1}) + V_{e_2}(\chi_{e_2}, \varsigma_{e_2}) + V_h(\chi_h, \varsigma_h) \\
&\left. + \frac{e^2}{4\pi\varepsilon\varepsilon_0} \left[\frac{1}{\sqrt{R^2\chi_3^2 + L^2\varsigma_3^2}} - \frac{1}{\sqrt{R^2\chi_1^2 + L^2\varsigma_1^2}} - \frac{1}{\sqrt{R^2\chi_2^2 + L^2\varsigma_2^2}} \right] \right\} \\
&\quad \times R^6 L^2 \chi_{e_1} d\chi_{e_1} \chi_{e_2} d\chi_{e_2} \chi_h \, dx_h d\varsigma_{e_1} d\varsigma_{e_2} d\varsigma_h y_h
\end{aligned} \tag{14}$$

The denominator in the R.H.S (normalization term) of equation (11) is:

$$\left\langle \Psi_{trion} \middle| \Psi_{trion} \right\rangle = \int_{-1}^{1}\int_{-1}^{1}\int_{-1}^{1}\int_{0}^{1}\int_{0}^{1}\int_{0}^{1} \left(f^2(\chi_{e_1}) f^2(\chi_{e_2}) f^2(\chi_h) g^2(\varsigma_{e_1}) g^2(\varsigma_{e_2}) g^2(\varsigma_h) \right) \times [\varphi(\chi_{e_1}, \chi_{e_2}, \chi_h, \varsigma_{e_1}, \varsigma_{e_2}, \varsigma_h)]^2 \times R^6 L^2 \chi_{e_1} d\chi_{e_1} \chi_{e_2} d\chi_{e_2} \chi_h dx_h d\varsigma_{e_1} d\varsigma_{e_2} d\varsigma_h \tag{15}$$

Substituting equations (14) and (15) in equation (11), we get the ground state energy of the trion (E_{trion}).

2.3. Positive trion

The positive trion (X^+) is created when an additional hole is bound to a pre-existing exciton (X), the positive Trion Hamiltonian can be obtained from equations (7) and (8) by interchanging the indices $e_2 \leftrightarrow h$ and ascribing the indices 1 and 2 to the holes.

$$\begin{aligned} H = {} & \frac{-\hbar^2}{2m^*_e}\left\{\frac{\partial^2}{\partial r_e^2} + \frac{1}{r_e}\frac{\partial}{\partial r_e} + \frac{\partial^2}{\partial z_e^2}\right\} \\ & \frac{-\hbar^2}{2m^*_h}\left\{\frac{\partial^2}{\partial r_{h_1}^2} + \frac{1}{r_{h_1}}\frac{\partial}{\partial r_{h_1}} + \frac{\partial^2}{\partial z_{h_1}^2}\right\} \\ & \frac{-\hbar^2}{2m^*_h}\left\{\frac{\partial^2}{\partial r_{h_2}^2} + \frac{1}{r_{h_2}}\frac{\partial}{\partial r_{h_2}} + \frac{\partial^2}{\partial z_{h_2}^{\,2}}\right\} \\ & + V_e(r_e, z_e) + V_{h_1}(r_{h_1}, z_{h_1}) + V_{h_{21}}(r_{h_2}, z_{h_2}) \\ & + \frac{e^2}{4\pi\varepsilon_0\varepsilon}\left[\frac{1}{\sqrt{(r_{h_1} - r_{h_2})^2 + (z_{h_1} - z_{h_2})^2}} - \right. \\ & \left. - \frac{1}{\sqrt{(r_{h_1} - r_e)^2 + (z_{h_1} - z_e)^2}} - \frac{1}{\sqrt{(r_{h_2} - r_e)^2 + (z_{h_2} - z_e)^2}}\right] \end{aligned} \tag{16}$$

By the same mathematical method that was done with the negative trion, we can have the energy of a positive trion (E_{trion}).

The binding energy of the charged exciton (negative or positive trion) is defined as:

$$E_b = E_i + E_{ex} - E_{trion} \tag{17}$$

Where E_i is the ground state energy of the free electron or the free hole [27], E_{ex} is the ground state energy of the exciton in the quantum dot as presented by equation (5), and E_{trion} is the ground state energy of the negative or positive trion calculated from equation (11).

3. Results and discussion

Applying this methodology for the GaAs cylindrical QD, we consider the following values of the confinement potential [13]: $V_o^e = 0.57(1.155x + 0.37x^2)eV$ for the electron and $V_o^h = 0.43(1.155x + 0.37x^2)eV$ for the hole. In our calculation, the Al concentration in the barrier material $Al_xGa_{1-x}As$ is taken as x. Furthermore, we used the following material parameters [13]: the relative dielectric constant for GaAs is $\varepsilon = 12.58$ and the effective masses are $m_e^* = 0.067m_o$, $m^*_h = 0.34m_o$ for the electron and the isotropic hole mass, respectively, where m_o is the mass of the free electron.

Figure (1) shows the calculated the exciton binding energy for the ground state as a function of the quantum dot radius for three different values of the width L/2 = 4, 7, and 10 nm. The calculated values show the presence of the well-known peaks of the binding energy curves in nanostructures, which depend strongly on the QD radius (R values), but its dependence on the QD width (L/2 values) is not strong. These results are in a good consistence with the previous data obtained by Le Goff and Stebe [41].

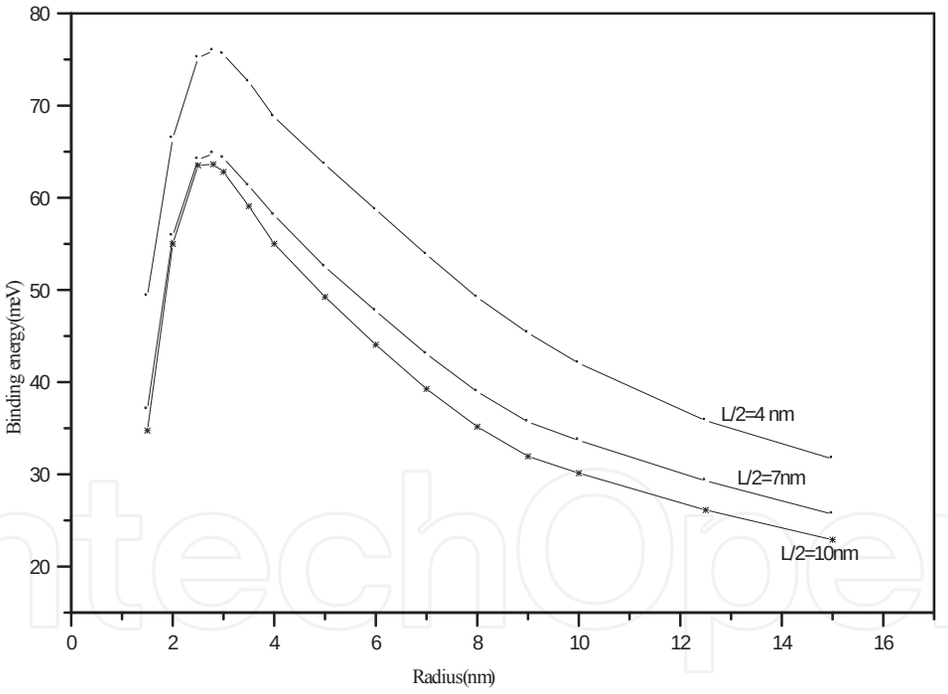

Figure 1. The binding energy of the exciton as a function of R. The Three curves are at different values of QD disc width L (as indicated).

Here, we would like to add that the peak positions of the binding energy as a function of L/2 also occur at almost one value of R = 3nm. We notice the sudden decrease of the exciton binding energy with the decrease in radius values. When R increases from 7-10nm, the binding energy changes almost by 10meV, and changes almost by half this value if the disc width L/2 increases from 7-10nm.

http://dx.doi.org/10.5772/61177

Figure (2) displays the variation of the exciton binding energy as a function of R, but for two different values of Al concentration (x= 0.15, 0.4). Here, a right shift of the peak position by almost 1nm and by 20 meV in height is observed when the quantity of Al increases by a ratio of 0.25. The height of the peak translated to higher values by increasing the barrier height (large x), which is due to the more confinement of the particles. Here, the position of the exciton binding energy peaks can be estimated to occur around L/2 ≅ 4nm and R ≅ 3nm or a diameter ≅ 6nm for the quantum dot disc.

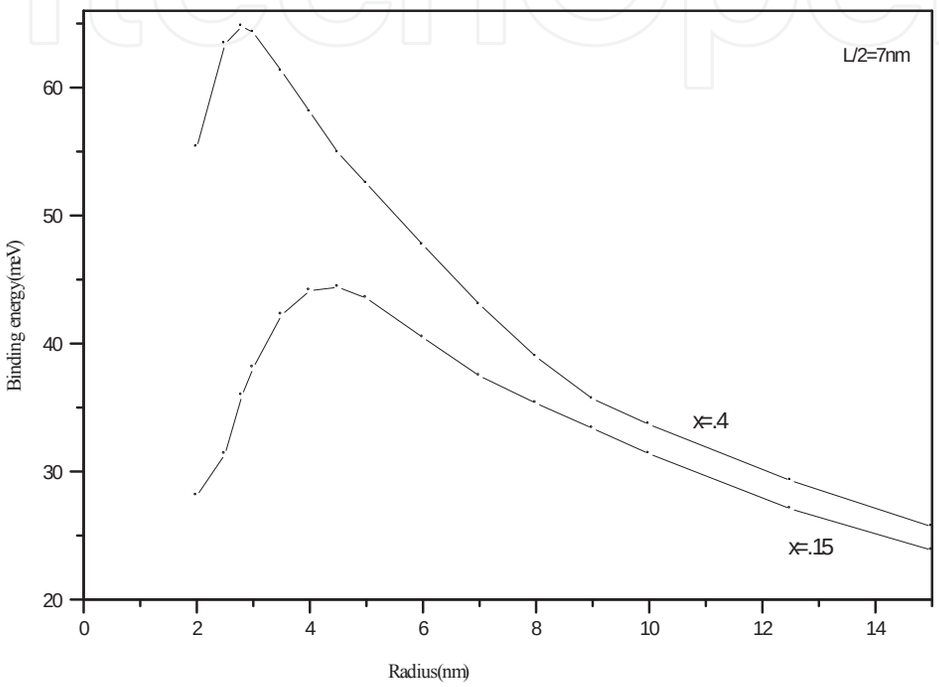

Figure 2. The variation of the exciton binding energy with R, At two different values of A1 concentration, x=0.15, and 0.4

It has been shown in reference (35) that there is a scaling rule for circular and square quantum wires of the form L/2R = 0.9136 such that a square wire of width L is equivalent to a circular wire of diameter 2R if the ratio of 0.9136 is achieved. Using this scaling rule, the critical confinement width for a quantum square wire of width L=5.4nm is equivalent to the present quantum disc with a radius R≅3nm. From the behavior of the binding energy positions discussed above, we may conclude that the bulk effect sets in along one spatial axis around L/2 ≅4.5 to 6nm, fairly independently of the confinement conditions. The present results should be useful for designers of nanoscale devices.

Concerning the discussion above about the quantum size effect, we present in figure (3) the exciton binding energy (E_b) and the corresponding exciton energy $\langle H \rangle$ as a function of the disc radius R at two different values of L/2 = 4,7, and 10nm.

In figure (3-a), there is no intersection between the exciton energy and the exciton binding energy ($\langle H \rangle / E_b > 1$) all the time so the exciton stability is small. At the intersection point figures

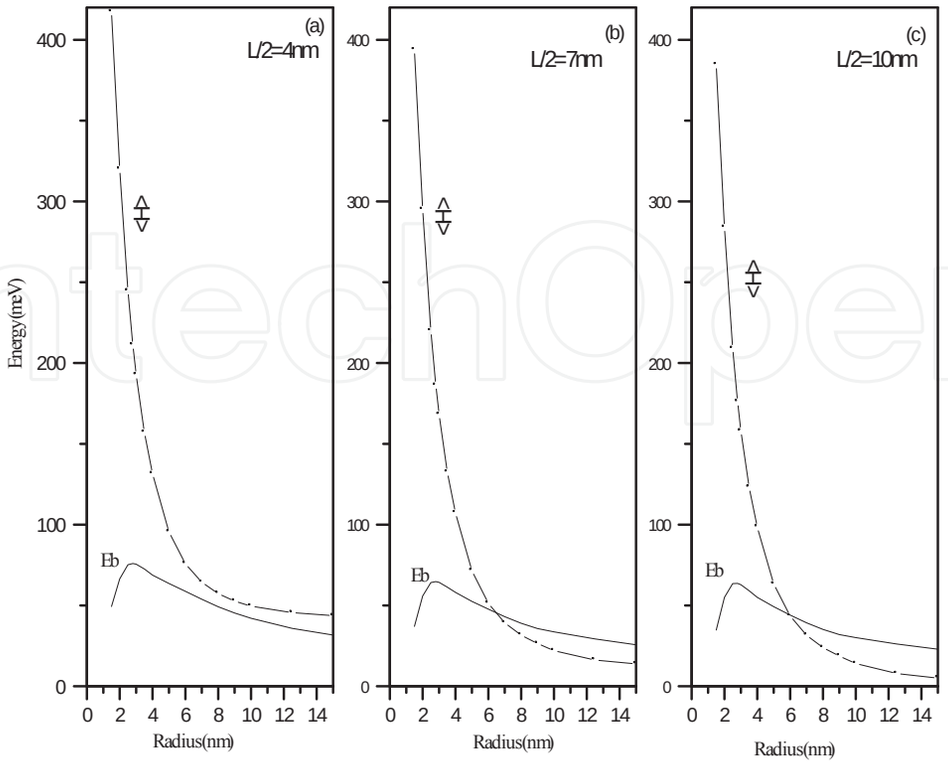

Figure 3. The exciton energy (<H>) and the exciton binding energy (Eb) versus the radius R. a) at L=4nm, b) at L=7nm, c) L=10nm.

(3-b and 3-c), we have the binding energy equal to the expectation value of the Hamiltonian and equal to half the free particles energy (E_e+ E_h). Before the intersection point where $\langle H \rangle / E_b > 1$, the exciton state directs to annihilation faster than after the intersection point where $\langle H \rangle / E_b < 1$. The crossover of the binding energy curve with the Hamiltonian curve confirms our above discussion. In order to obtain a large exciton binding energy, we should choose quantum dots with radius from 3nm to 10nm. However, if the radii of quantum dots are beyond the nanostructure scale, the principle of quantum theory is unavailable and the electronic properties of dots belong to the region of bulk materials.

One of main goals of this chapter is to estimate the best theoretical model with an available data to fit, and to clarify the paradoxes about the trion binding energy, which are discussed in previous researches. Since the available existing experimental data are given in the work of Backer et al. [42], to match our parameters with theirs we therefore used the anisotropic hole effective mass (hole effective mass in the z-direction (m^*_{hz}) is different from its value in the in-plane direction $\left(m^*_{hxy}\right)$, such as: $m^*_{hz}=0.377m_o$ and $m^*_{hxy}=0.112m_o$). The results of the charged exciton binding energies as a function of the half-height (L/2) of the QD are shown in Figure (4) and are evaluated at x = 0.3 with a QD radius (R) equal to 15 nm. The curves with solid squares and solid circles correspond to our theoretical calculations of the negatively charged exciton binding energy (E_b^-) and positively charged exciton (E_b^+), respectively, whereas, the opened square points and opened circle points indicate the experimental values of the binding

http://dx.doi.org/10.5772/61177

energies [42] of the negative and positive trion, respectively. For each curve, we see that the binding energy increases as the dot half height decreases, which leads to the trions being more stable at small QD (strong confinement regime). When the half-height becomes greater than the effective electron Bohr radius for Ga As (a_B=9.9 33 nm), the binding energy of X^- decreases rapidly and reaches values less than the binding energy of X^+. At a small QD size, the gain of the binding energy as a function of the size of QD comes from the Coulomb interaction related to the distances of the interparticles where the Coulomb interaction between the electrons (V_{ee}) in X^- is larger than the Coulomb interaction between the holes (V_{hh}) in X^+, and the Coulomb interaction at this size is more effective than the massive localization of the system, so $E_b^- > E_b^+$. Our theoretical values for both trions are shifted approximately by 0.3 meV (7%) from the experimental value.

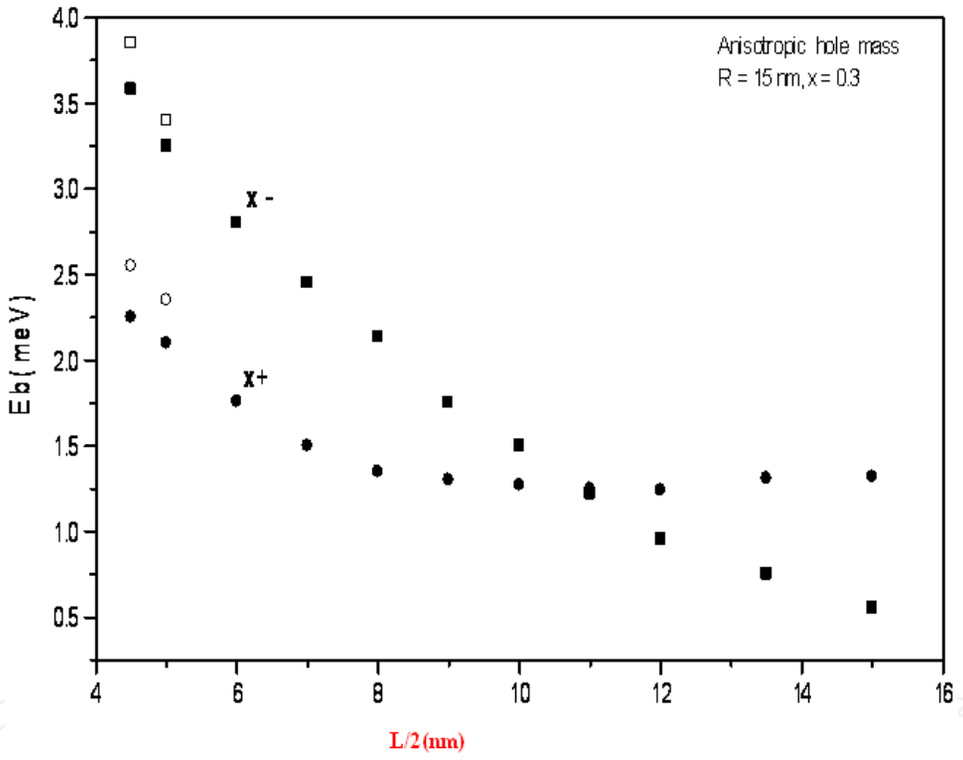

Figure 4. Trion binding energy (E_b) as a function of QD half-height (L/2) at radius R=15 nm, for an anisotropic effective hole mass. The closed circles and closed squares represent the theoretical results of (E_b^+) and (E_b^-), respectively. The experimental data for (E_b^+) and (E_b^-) are indicated by opened circles and opened squares, respectively.

In table (1), we summarize our theoretical results, compared with the experimental data and other theoretical data calculated by using the Path Integral Monte Carlo method (PIMC) (Ref (42)). Table (1-a) and Table (1-b) show the negative and the positive trion data, respectively.

We refer the acceptable agreement between our theoretical and the experimental data to the following two issues. The first issue is that we considered a theoretical model that solved a full

L/2 (nm)	Ours $E_b(x^-)$ meV	Exp. (meV) Ref [42]	Value(%) shift from Exp.	PIMC meV) Ref [42]	Value(%) shift from Exp.
4.5	3.6	3.9	7.69%	2.9	25.6%
5	3.25	3.4	4.41%	2.5	26.47%

(a)

L/2 (nm)	Ours $E_b(X^-)$ meV	Exp. (meV) Ref [42]	Value (%) shift from Exp.	PIMC (meV) Ref [42]	Value(%) shift from exp.
4.5	2.27	2.6	12.69%	2.25	13.46%
5	2.22	2.4	7.5%	2.0	8.33%

(b)

Table 1. (a): The negative trion results; (b): The positive trion results.

3-D confinement of the trions inside the QD; the second issue is the choice of the trial wave function, which describes correctly the internal motion of the trion. Let us discuss the binding energy of the charged excitons confined inside a cylindrical QD, with an isotropic hole effective mass $\left(m^*_h = 0.34\, m_o\right)$.

We have calculated the negatively charged exciton binding energy (E^-_b solid squares) and the positively charged exciton binding energy (E^+_b solid circles) as a function of the QD half-height. The results are shown in figure (5) and are calculated at x = 0.3 and R=15nm. Also, we obtained a more stable negative trion system than the positive trion system at small QD. Besides, E^-_b crosses down E^+_b at a larger value of the QD half-height (L/2=15nm) than in the case of an anisotropic hole effective mass (L/2=11nm).

Now, we come to the second goal of our work on trions, which concerns the paradoxes existing in most of the previous papers. In Refs (42, 43, and 44), the authors obtained a higher binding energy of the negative trion than the positive one over all of the QD dimensions they examined. On other hand, the demonstrated data in Refs (18 and 38) showed that the binding energy of the negative trion is less than the binding energy of the positive trion. In Ref (18), the author introduced the correlated hyperspherical harmonics as basic functions to solve the hyper angular equation for negative and positive trions in a harmonic quantum dot. He introduced, as an approximation of the center of mass coordinates, to reduce the variables and consequently simplified the calculations. In Ref (38), the authors formulated the Hartree-Fock approximation using a calculation method, which is based on the quantum adiabatic theorem, to study the stability of the charged excitons in QD. Again, we see that the standard tools of the condensed-matter physics, like the many body techniques relying on the Hartree-Fock approximation, are often not sufficient since the exchange and correlation energies can notare not negligible [45]. The full three dimensional calculation is introduced by Szafran et al. [23] for a trion confined in a spherical quantum dot, and the authors found that the binding energy of the negative trion is less than the binding energy of the positive trion at a large radius and vice versa at a small radius. Generally, this agrees with our view. The results shown in figure

(5) coincide with the results given in Refs. 42, 44, and 45. Here, $E_b^- > E_b^+$ as long as the QD size is small. Also, our results are qualitatively similar to those obtained by the authors in Refs. 18 and 38 in the case of a large QD size where they showed that $E_b^+ > E_b^-$ as given in figure (6).

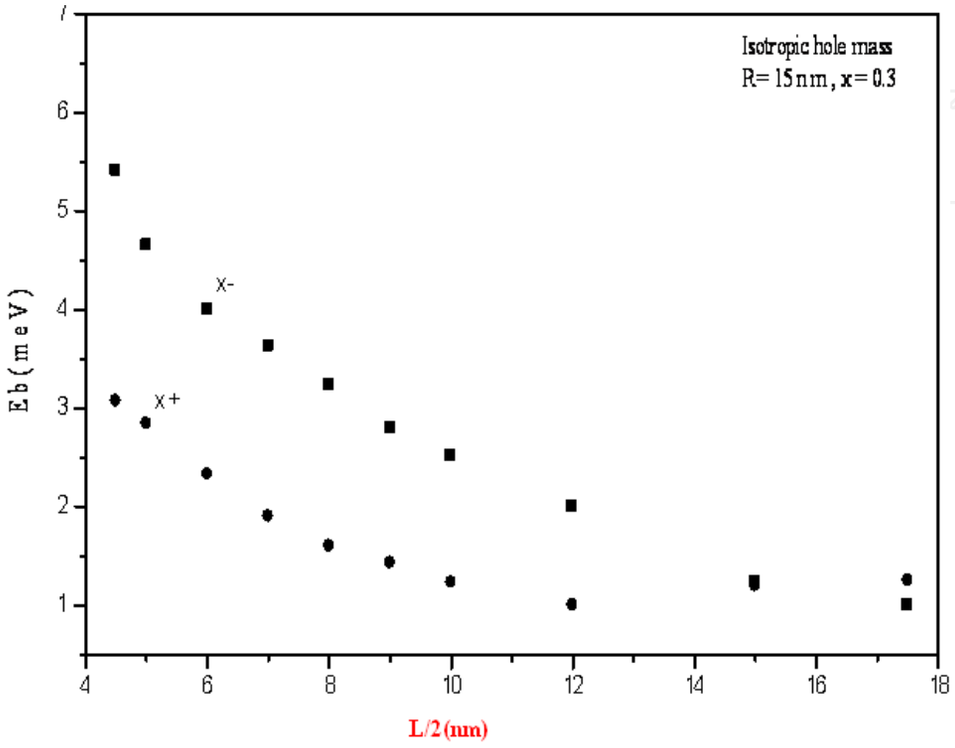

Figure 5. The variation of trion binding energy (E_b) calculated as a function of QD half-height (L/2) at a radius of R=15 nm, for an isotropic hole mass. The closed circles correspond to E_b^+ of positive trion and the closed squares correspond to E_b^- of negative trion.

The possibility to observe negative or positive trions depends on its stability against dissociation into an exciton and free electron or hole. The corresponding sufficient stability condition for the charged excitons is [38] $E_b^{\pm} \geq 0$. Concerning the stability of X^- and X^+ in the case of isotropic and anisotropic hole effective mass, from figures (4) and (5), we observe that the positive and negative trions are stable, while from figure (6), X- is unstable in a large QD (L >2 a_B) and X^+ is stable even near the bulk limit.

In order to get a physical insight into the stability of X^+ at large QD size, this can be attributed to its heavy mass. This heavy mass system becomes more localized and stable even inside large QDs. As a result, the positive trions binding energy behavior allowed most of experimentalists to detect X^+ near room temperature in such large dimensional structures.

At last, a comparison between the ground state energy and the binding energy of the positive and negative trions and the excitons is shown in figure (7). In figure (7- a), the ground state energies of the trions X^-, X^+, and exciton (X) are plotted as a function of the QD half-height (L/2) for the isotropic hole mass. Similarly, the binding energies are shown in figure (7-b). From

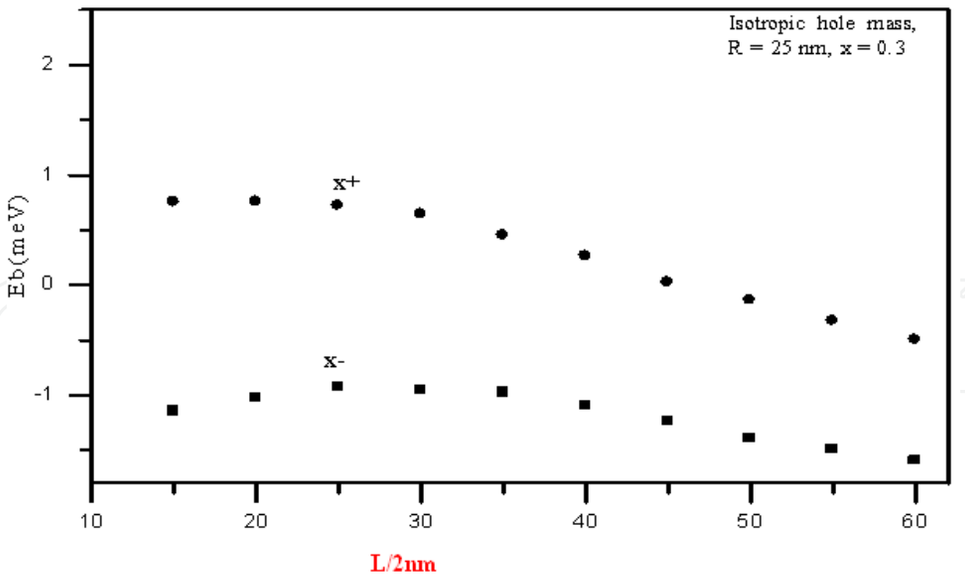

Figure 6. The trion binding energy as a function of L/2 at R=25 nm for an isotropic effective hole mass. Closed circles correspond to the positive trion and closed squares correspond to the negative trion.

this figure, one can see that the neutral exciton has the lowest ground state energy (E^X) compared to that of the trions $(X^-,\ X^+)$(figure7-a).

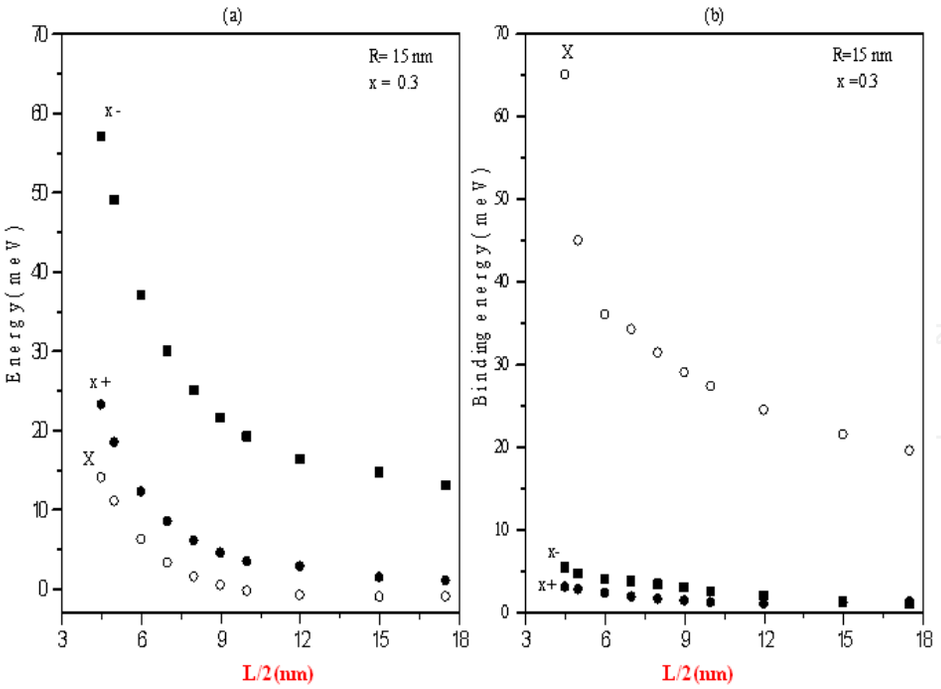

Figure 7. a) Exciton (X) and charged excitons $(X^-$ and $X^+)$ ground state energies as a function of QD half-height L, at radius R= 15 nm. b) The binding energies of exciton and charged excitons as a function of QD half-height L/2.

http://dx.doi.org/10.5772/61177

Also, we notice that it decreases monotonically and not rapidly like the trions ground state energies. In other words, within the examined range of the QD height, we obtained a drop in E^X by 14 meV, while E^{X^+} decreased by 22meV and E^{X^-} decreased by 44meV. By looking at figure (7-b), one can see that the exciton is the most stable system. For small QDs, this stability (or the largest binding energy) of X may be referred as the strong confinement regime of the QD where the exciton is severely restricted in all spatial directions and the quantum confinement are at a maximum for this system. Defining the neutral exciton binding energy $(E_b{}^X)$ in the same manner as in equation (6) $\{E_b{}^X = E_e + E_h - E^X\}$, we find that E^X is the lowest but not comparable to the single particles ground state energy. However, for positive and negative trions, their ground state energies compete with the single particle, where E^{X^-} is larger and comparable with E_e, but E^{X^+} competes with E_h, therefore their binding energy is low compared to the neutral exciton. Within the examined QD size, we obtained a drop by 45, 4 and 2 meV in the binding energy of X, X^-, and X^+, respectively. The decrease of the exciton binding energy seems dramatic, but compared with the trions it is not. The binding energy of the negative trion drops by 80% when the QD half-height changes from 4.5nm to 18nm, while $E_b{}^X$ and $E_b{}^+$ within the same size range decrease by 70% and 55%, respectively.

4. Conclusion

We have introduced a trial wave function for the positive and negative trions confined in a cylindrical QD. Using the given wave, we obtained a higher binding energy of negative trions than the positive trions inside the QD with a half-height less than the effective Bohr radius and we referred that to the high Coulomb interaction energy between the two electrons compared to the weak Coulomb interaction between two holes at such small QDs. When the half-height of the QD increased to values higher than the Bohr radius, the negative trion binding energy rapidly decreases than the binding energy of the positive trion. An anisotropic hole effective mass state is demonstrated to compare our model with the experimental results. We obtained a good agreement with the experimental results up to 0.3 meV (7%). To improve the stability of the trions $(X^-,\ X^+)$, in such structures, it is necessary to operate with a special QD size, which permits an enhancement of the binding energy.

5. Appendix

We want to prove the formula that given in equation (13)

$$\left\langle \psi^* \right| - \left(\frac{d^2}{dr^2} + \frac{1}{r}\frac{d}{dr} \right) \left| \psi \right\rangle = \int_0^\infty \left(\frac{d\psi}{dr} \right)^2 r dr \tag{18}$$

Proof

$$\because \left\langle \psi^* \right| - \left(\frac{d^2}{dr^2} + \frac{1}{r}\frac{d}{dr} \right) \left| \psi \right\rangle = -\int_0^\infty \Psi^* \left\{ \frac{d^2}{dr^2} + \frac{1}{r}\frac{d}{dr} \right\} \psi \, r dr \tag{19}$$

Let

$$I = -\int_0^\infty \Psi^* \left\{ \frac{d^2}{dr^2} + \frac{1}{r}\frac{d}{dr} \right\} \psi \, r dr = -\int_0^\infty \Psi^* \frac{1}{r}\frac{d}{dr}\left(r\frac{d}{dr}\right) \psi \, r dr \tag{20}$$

where ψ is a real eigenfunction.

From equation (3)

$$I = -\int_0^\infty \Psi^* \frac{d}{dr}\left(r\frac{d}{dr} \right) \psi \, dr \tag{21}$$

But from the integration methods we can use the fact that

$$\int u\,dv = uv - \int v\,du \tag{22}$$

Let

$$u = \Psi^* \Rightarrow du = \frac{d\Psi^*}{dr} dr \text{ and } dv = \frac{d}{dr}\left(r\frac{d\psi}{dr}\right) \; v = \left(r\frac{d\psi}{dr}\right) \tag{23}$$

By using equation 5 and 6 and substituting in equation 4

$$\therefore I = -\left[\psi^* r \frac{d\psi}{dr} \right]_0^\infty + \int_0^\infty r\frac{d\Psi}{dr}\frac{d\psi^*}{dr} \, dr \tag{24}$$

But $\left[\psi^* r \frac{d\psi}{dr} \right]_0^\infty = 0$ because $\psi(\infty) = 0$ (real eigenfunction condition)

$\because \psi$ is a real function $\Rightarrow \psi^*\psi = \psi^2$, $\frac{d\Psi}{dr}\frac{d\psi^*}{dr} \Rightarrow \left(\frac{d\Psi}{dr}\right)^2$.

This means we can rewrite equation (7) as

$$I = \int_0^\infty r \frac{d\Psi}{dr} \frac{d\psi^*}{dr} dr = \int_0^\infty \left(\frac{d\Psi}{dr} \right)^2 r\, dr \tag{25}$$

From equation 2, 3, and 8, relation 1 is proven.

Author details

S. A. Safwan* and N. El–Meshed

*Address all correspondence to: safwan_s_2000@yahoo.com

The Theoretical Physics Department, National Research Center, Cairo, Egypt

References

[1] Jacques I. Pankove, Optical Processes in Semiconductors, Prentice-Hall, Inc. (1971).

[2] L.V.Keldy, P.N.Lebedev, Contemp.Phys.27,395(1986).

[3] M.A. Lampert, Phys. Rev.Lett.1, 450(1958).

[4] G. Finkelstein, V.Umansky, and I. Bar-Joseph, Phys. Rev. B58, 12637(1998).

[5] Peter Ramvall, Satoru Tanaka, Philippe Riblet, and Yoshinobu Aoyagi.,Appl.Phys.Lett. 73,1104(1998).

[6] L. Esaki, in physics and Application of Quantum wells and superlattice, vol 170, of NATO Advanced study institute, series B: physics, edited by E.E, Mendez and K.von klitzing (plenum, new York, 1987).

[7] K. Kheng, R.T. Cox, Merle Y. dÁubigne, Franck Bassani, K. Saminadayar and Tatarennko, Phys.Rev.Lett. 71, 1752(1993).

[8] G. Finkelstein, H. Shtrikman, and I. Bar-Joseph, Phys. Rev. Lett.74, 976(1995).

[9] A. J.Shields M. Pepper, D. A. Ritchie, M. Y. Simmons and G. A. C. Jones, Phys. Rev. B51,18049(1995).

[10] D. Sanvitto, F. Pulizzi, A.J. Shields, P.C. Christianen, S. N. Holmes, M.Y. Simmons, D. A. Ritchie, J. C. Maan, and M. Pepper, Science 294, 837(2001).

[11] G.Eyton, Y. Yayon, M. Rappaport, H. Shtrikman, and I. Bar-Joseph., Phys. Rev. Lett. 81,1666(1998).

[12] Y. Yayon, M. Rappaport, V. Umansky and I. Bar-Joseph, Phys. Rev. B64, 81308(2001).

[13] C. F. Lo and R. Sollie, Solid state commun 79,775 (1991)

[14] S. I. Pokutnil, Fiz Tekh Poluprovodn,Sov.phys. Semicond 25, 381 (1991)

[15] G. T.Einevoll, Phys. Rev. B45, 3410 (1992).

[16] M.A. Olshavsky, A. N. Goldstein, and A. P. Alivisatos, J. Am. Chem.Soc.112, 9438 (1990).

[17] W. Xie, and C. Chen, Physica E 8, 77 (2000).

[18] W.F. Xie, Phys.Stat.Sol. B226, 247(2001)

[19] B.Stebe, A.Moradi, and F. Dujardin, Phys. Rev. B61, 7231(2000).

[20] C.Riva F. M. Peeters, and K. Varga, Phys. Rev. B61, 13873(2000).

[21] I. Szlufarska, A. Wojs, and J. J. Quinn, Phys. Rev. B63, 085305 (2001).

[22] W.Y.Ruan, K. S. Chan, and, E. Y. B. Pun, J. Phys.: Condens. Matter 12, 7905(2000).

[23] B.Szafran, B. Stebe, J. Adamowski, and S. Bednarek, J. Phys.: Condens. Matter 12, 2453 (2000).

[24] L. C. O. Dacal and J. A.Brum, Phys. Rev. B65,115324 (2002).

[25] I. M. Kupchak,Yu. V. Kryuchenko, and D. V. Korbutyak, Semiconductor Physics, Quantum Electronics & Optoelectronics, V.9, N1, P 1-8 (2006).

[26] J.L.Marn, R.Riera, and S.A.Cruz, J. Phys: condens. Matter 10,1349(1998).

[27] Shudong Wu and Liwan, J. Appl. Phys.111,063711(2012).

[28] H.Hassanabadi and A.A.Rajabi, Phys. Lett. A373,679,(2009).

[29] L.C.Lew Yan Voon and M. Willatzen, J. Phys: Condens. Matter 14,13667(2002).

[30] S.Gaan, Guowei, and R. Feenstra, J. Appl. Phys 108,114315 (2010).

[31] G. W. Bryant, Phys. Rev. Lett.59, 1140 (1987).

[32] G. W. Bryant, Phys. Rev. B37, 8763 (1988)

[33] Y.Kayanuma, Phys. Rev. B44, 13085 (1991).

[34] V.A. Holovatsky, M.J. Mikhalyova, and M.M. Tkach. J. Phys.: Condens. Matter 3,863(2000).

[35] J. Marin, L. Riera, and S. A. Cruz, J. phys. Condens matter 10, 1349 (1998).

[36] Tong San Koh,Yuan Ping, and H.N.Spector, J. Phys.: Condens. Matter 13,1485(2001).

[37] M.H. Hekmat, Nagwa A. Elmeshad, and S. A. Safwan, Fizika A 13, 1(2004).

[38] S. Baskoutas and A.F. Terzis, Micro. Eng. 81, 61(2005).

[39] A. A. Guzelian, U. Banin, A. V. Kadavanich, X. Peng, and A. P. Alivisatos, Appl. Phys. Lett.69,1432(1996).

[40] W. F. Xie and C. Y. Chen, Solid State Commun.107, 439(1998).

[41] S. Le Goff and B. Stebe, Phys. Rev. B47, 1383 (1993).

[42] A.S.Bracker, E.A. Stinaff, D. Gammon, M. E. Ware, J.G. Tischler, and D. Park, Phys. Rev. B72, 035332(2005).

[43] B.Szafran, B.Stebe, J.Adamowski, and S.Bednarek, Phys. Rev. B66, 165331 (2002).

[44] V.Regelman, D.Gershoni, E.Ehrenfreund, W.V.Schoenfeld, and P.M.Petroff, Physica, E13, 114(2002).

[45] D. Pfannkuche, V.Gudmundsson and P.A.Maksym, Phys. Rev. B47, 2244(1993).

IntechOpen